Self-Assembled Phenylethynylene Bis-urea Macrocycles Facilitate the Selective Photodimerization of Coumarin

Sandipan Dawn,[†] Mahender B. Dewal,[†] David Sobransingh,[†] Monissa C. Paderes,[†] Arief C. Wibowo,[†] Mark D. Smith,[†] Jeanette A. Krause,[‡] Perry J. Pellechia,[†] and Linda S. Shimizu*,[†]

[†]Department of Chemistry and Biochemistry, University of South Carolina, Columbia, South Carolina 29208, United States
[‡]The Richard C. Elder X-ray Crystallographic Facility, Department of Chemistry, University of Cincinnati, Cincinnati, Ohio 45221, United States

S *Supporting Information*

ABSTRACT:

Porous nanotubes — Selective dimerization
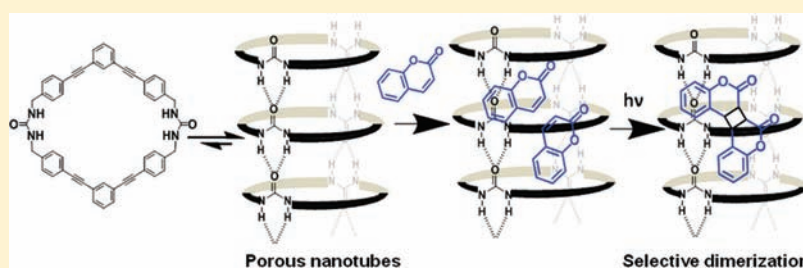
There is much interest in designing molecular sized containers that influence and facilitate chemical reactions within their nanocavities. On top of the advantages of improved yield and selectivity, the studies of reactions in confinement also give important clues that extend our basic understanding of chemical processes. We report here, the synthesis and self-assembly of an expanded bis-urea macrocycle to give crystals with columnar channels. Constructed from two C-shaped phenylethynylene units and two urea groups, the macrocycle affords a large pore with a diameter of ∼9 Å. Despite its increased size, the macrocycles assemble into columns with high fidelity to afford porous crystals. The porosity and accessibility of these channels have been demonstrated by gas adsorption studies and by the uptake of coumarin to afford solid inclusion complexes. Upon UV-irradiation, these inclusion complexes facilitate the conversion of coumarin to its *anti*-head-to-head (HH) photodimer with high selectivity. This is contrary to what is observed upon the solid-state irradiation of coumarin, which affords photodimers with low selectivity and conversion.

■ INTRODUCTION

Chemists do not normally think twice about the flask when setting up a new reaction. Yet the container can dramatically influence molecular processes. Nanocapsules,[1] zeolites,[2] and sol—gels[3] have been used as molecular sized flasks to influence the properties, stability, and even the reactivity of absorbed or encapsulated molecules. Encapsulation has been shown to enhance the stability of unstable molecules.[4] For example, molecular sized containers stabilized carbocations and enabled chemists to probe their structure.[5] Encapsulation can be used to modulate reactivity and dramatically change product distributions.[6] Zeolites in particular can be used to selectively afford products that are not observed in solution.[7] On top of the advantages of improved yield and selectivity, the studies of reactions in confinement also give important clues that extend our basic understanding of chemical processes. We report herein, the synthesis and self-assembly of a new molecular container, a phenylethynylene bis-urea macrocycle **1**. This macrocycle assembles into columnar structures to yield porous crystals with channels with diameters of ∼9 Å. We demonstrate the accessibility of these channels by gas adsorption studies, characterize their

inclusion complexes (Figure 1), and show their utility as confined environments for a selective photochemical reaction of coumarin.

Our group is interested in synthesizing porous materials with homogeneous channels for use as confined reaction environments. Specifically, we have used macrocycles that contain two rigid spacers and two urea groups, which self-assemble into straw-like structures guided by the formation of 3-centered urea—urea hydrogen bonds between the neighboring macrocycles as well as by the formation of favorable aryl stacking interactions.[8] The size of the open cylindrical channel is controlled by the size and shape of the macrocyclic building blocks. Thus far, we have used benzophenone and phenylether as spacers to generate macrocycles. These spacers are very similar in size and generate porous materials with channels of ∼6 Å that can be used to facilitate photochemical reactions.[9] Herein, we report the use of phenylethynylene spacers that are nearly double the length of the prior systems (Figure 2). We investigated the ability of two ureas to guide the assembly of these larger macrocycles
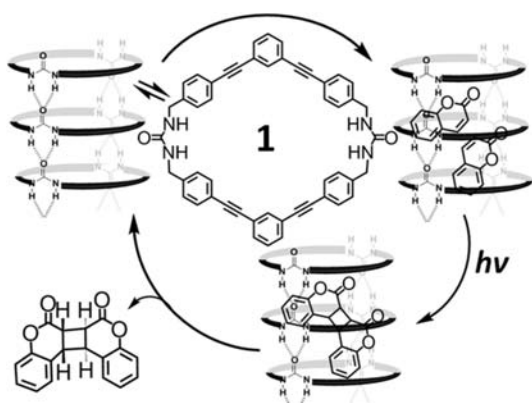
Figure 1. Bis-urea macrocycles were designed to self-assemble into columns affording accessible channels. Uptake of coumarin from solution yields a solid host–guest complex. Broad-band UV-irradiation of the complex selectively affords the *anti*-head-to-head photodimer.
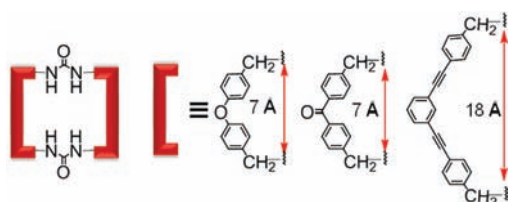

Figure 2. Comparison of the relative length of rigid spacers used to construct macrocyclic bis-ureas.

with high fidelity into columnar structures from two different solvents and characterized the solid-state assembled structures. The porosity of these materials was evaluated by gas adsorption and guest uptake studies. Finally, the utility of these larger channels was demonstrated by their ability to facilitate the photodimerization of coumarin under UV-irradiation.

■ RESULTS AND DISCUSSION

The phenylethynylene spacers are of interest due to their larger length and conjugated nature. Substituted poly *para*-phenylethynylenes have demonstrated applications in optical/fluorescence based sensing of substrates of biological interest[10] including DNA.[11] Oligomers of *meta*-phenylethynylenes fold into helical structures[12] or can be cyclized to give macrocycles such as those reported by Moore,[13] Hoger,[14] and others.[15] Moore's shape persistent arylene ethynylene macrocycles assembled into fibrils that displayed polarized emission parallel to the stacking direction.[16] Such emission is indicative of intermolecular delocalization of the electrons in the pi clouds. Thus, columnar assembled phenylethynylene derivatives may have applications as sensors, semiconductors, and photovoltaic devices. Our long-term goal is to evaluate if the urea assembly motif could augment that of phenylethynylenes to afford a larger macrocyclic cavity that upon assembly would give porous materials that combine molecular recognition properties with the electronic characteristics of the component phenylethynylenes.

Macrocycle **1** was synthesized in four steps from commercial 1,3-diethynylbenzene using a Sonogashira–Hagihara coupling with excess 4-iodobenzyl alcohol to yield the diol spacer, which was subsequently converted to the dibromide (Scheme 1). A

Scheme 1. Synthesis of Macrocycle 1[a]
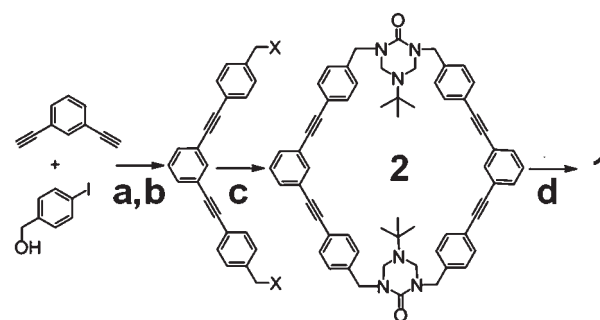
[a] Reagents and conditions: (a) Pd(PPh$_3$)$_2$Cl$_2$/ CuI/piperidine, 0 °C, 3 h, 97%; (b) NBS/PPh$_3$ in THF, 0 °C, 12 h, 87%; (c) triazinanone, NaH/THF, reflux 48 h, 22%; (d) 1:1 MeOH:(20% NH(CH$_2$CH$_2$OH)$_2$ in H$_2$O, pH ∼2), reflux 12 h, 96%.

macrocyclization with triazinanone under basic conditions, followed by deprotection, afforded the bis-urea macrocycle as a white precipitate. Microneedles of **1** (∼20 μm × 3 μm) were regularly obtained from hot DMSO (50 mg/10 mL) at 120 °C solution by slow cooling (1 °C/h) and were used for all the photochemical experiments. Larger pale yellow needles (0.20 × 0.05 × 0.04 mm^3) of similar morphology were obtained by slow cooling from 2:8 DMSO/nitrobenzene (30 mg/12 mL) and were subjected to a synchrotron X-ray diffraction study.

The X-ray crystal structure revealed the desired macrocycle and encapsulated but disordered nitrobenzene solvent (Figure S26 Supporting Information), which was omitted for clarity in Figure 3a. Despite their greater size, the phenylethynylene macrocycles assembled into columns very similar in structure to the smaller macrocyclic bis-ureas.[8,9] The individual macrocycles were organized into columns through the characteristic three centered urea hydrogen bonds, which displayed (N)H···O distances of 2.06(3) and 2.20(3) Å respectively (Figure 3b). Additional stabilization was provided by edge to face aryl stacking and by stacking interactions between the alkyne and the phenyl on the neighboring macrocycle. The three phenyl rings in one-half of the macrocycle are independent by symmetry. One of the rings (ring z, Figure 3b) is disordered in a 50/50 ratio over two orientations (one orientation omitted for clarity). Two adjacent z and z′ rings provide stabilizing edge-to-face aryl interaction. Additional interactions between the alkyne and neighboring phenyl groups further stabilize the assembled columns. One of the triple bonds is packed closely to phenyl rings on adjacent macrocycles with distances of 3.49 and 3.38 Å, respectively (Figure 3c). Figure 3d highlights the view down the crystallographic *b* axis of seven hydrogen bonded tubes with the guests removed. Without the entrapped nitrobenzene, the calculated void volume is 491.1 Å^3 per unit cell (21% of the total unit cell volume). Individual columns are close packed together with benzene rings alternating tilt direction in the neighboring rows of tubes (Figure 3d).

Thermogravimetric analysis (TGA) was used to investigate whether the nitrobenzene solvent could be removed from the crystals. Host **1**·nitrobenzene displays a one-step desorption curve with a weight loss of 13.9% between 70 and 140 °C (Figure 4a). From the percent weight loss, we calculated the macrocycle:guest stoichiometry as 1:0.89 (calculated weight loss, 14.1% for a 1:0.94 complex). In comparison, the host **1**·DMSO crystals displays a two-step desorption curve from 30 to 170 °C with weight loss of 18.38% (Figure 4a). The two-step desorption
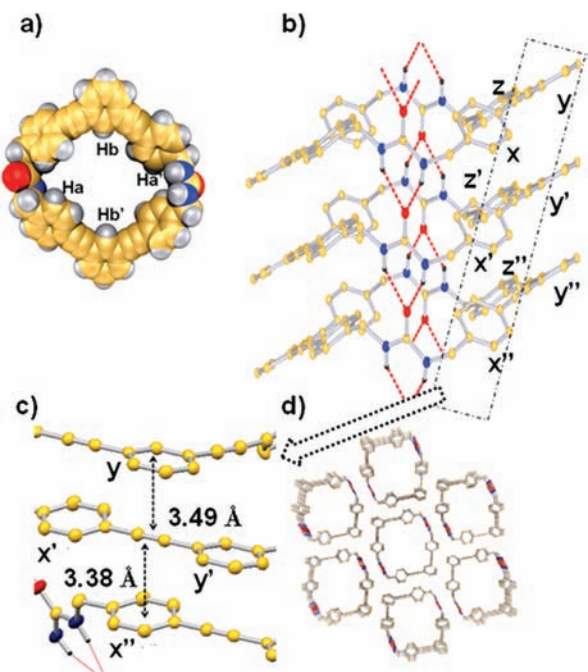
7026

dx.doi.org/10.1021/ja110779h |*J. Am. Chem. Soc.* 2011, 133, 7025–7032

Figure 3. X-ray structure of **1** $C_{50}H_{36}N_4O_2 \cdot (C_6H_5NO_2)_{0.94}$: (a) space filling view of a single macrocycle with intramolecular distances from Ha to Ha′ of ∼8.7 Å and Hb to Hb′ of ∼8.4 Å; (b) view alongside a single column that was organized via NH···O hydrogen bonds that run along the crystallographic *b* axis (nitrobenzene guests and hydrogens omitted); (c) expansion highlighting the alkyne···$\pi_{centroid}$ ring distances; (d) view down the *b* axis of seven H-bonded tubes (nitrobenzene guests omitted).
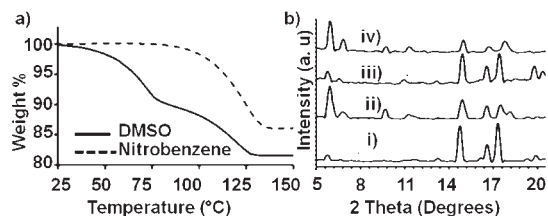

Figure 4. (a) TGA desorption curves for the host **1**·nitrobenzene (dashed line) and host **1**·DMSO (solid line). (b) PXRD comparison of crystals obtained from different solvents before and after heating: (i) from nitrobenzene before heating, (ii) from nitrobenzene after heating, (iii) from DMSO before heating, (iv) from DMSO after heating.

curve suggests that the DMSO is absorbed in two different environments within the crystals. From the measured total weight loss, we calculated a 1:2 host/guest stoichiometry. The average total weight loss for 12 different sizes and batches of crystals was 18.3%, with an 8.2% weight loss observed between 30 and 80 °C and 10.1% between 80 and 130 °C. The reproducible nature of the DMSO desorption from different sizes and batches of crystals experimentally suggests that the DMSO solvent is incorporated into the crystals and not adsorbed on the surface, much like nitrobenzene.

We turned to powder X-ray diffraction (PXRD) to compare the structure of these two crystalline forms of host **1** (**1**·nitrobenzene versus **1**·DMSO) and their solvent free forms. Host **1**·nitrobenzene crystals were ground to powder and examined by PXRD (Figure 4b, i). The experimentally observed PXRD pattern is nearly identical to the PXRD pattern simulated from the crystal
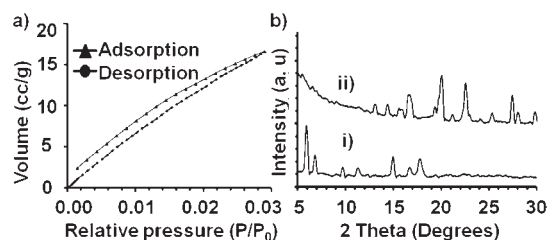

Figure 5. (a) CO_2 adsorption isotherm of host **1** at 273 K. (b) PXRD pattern of host **1** before (bottom) and after coumarin (**3**) absorption (top).

structure using POUDRIX,[17] suggesting that the bulk powder was similar in structure to the crystals. The guest was removed by TGA and the powder re-examined by PXRD (Figure 4b, ii). The PXRD shows a similar sharp and intense PXRD pattern, indicating that the empty host maintains long-range crystalline order after removal of the solvent. Next, the microcrystals of host **1**·DMSO were ground to a powder and examined by PXRD (Figure 4b, iii). The sharp and intense peaks in the powder pattern of host **1**·DMSO closely match those observed for host **1**·nitrobenzene, which suggests that it also has similar highly ordered crystalline structure (Figure 4b, i and iii). The DMSO guest was removed by heating. The empty structure displays peak positions and intensities that are in good agreement with the empty host generated from the nitrobenzene derived crystals (Figure 4b, ii and iv) suggesting that the empty frameworks assembled from the two different solvents have similar structures.

Single crystal data on host **1**·nitrobenzene suggests that the solvent-free structure could have open channels for binding guests. PXRD studies further support the hypothesis that host **1** adopts similar structures when assembled from different solvents (DMSO vs nitrobenzene). We next turned to gas adsorption to evaluate the porosity of the evacuated hosts. The solvent was removed from the abundant microcrystals obtained from DMSO by heating and the empty host (47 mg) was subjected to gas adsorption measurements. Host **1** shows a 6.6 mL/g CO_2 uptake at relatively low pressure (<0.03 atm). The adsorption isotherm reveals a steep rise at relatively low pressure, type I behavior that is typical for microporous materials (Figure 5a). The Brunauer−Emmett−Teller (BET) method was applied to the isotherm to calculate surface area.[18] The isotherm gave an apparent surface area of 349 m^2/g at 273 K between 0.010 and 0.028 relative pressures. The total pore volume was estimated as 0.025 cm^3/g at 273 K for pores smaller than 11.3 Å in diameter at $P/P_0 = 0.027$.

We next sought to load guests into these porous crystals by soaking the solid host in a solution containing the guest.[19] The guest was removed from the host **1**·DMSO crystals by heating and the free host (30 mg) was soaked in a coumarin **3** solution (0.1 mM in CH_3CN) for 1−12 h. The depletion of coumarin from solution was monitored by UV−vis (273 nm) and reached an equilibrium within 3 h (Supporting Information). A Lambert−Beer plot with variable concentration (0.01−0.1 mM) of coumarin in acetonitrile was used to calculate the ratio of host **1** to coumarin in the treated samples. The host/guest ratio was calculated as 1:1.4 and was found to be reproducible for different sizes and batches of host **1** crystals. The reproducible uptake of coumarin suggests that the coumarin guests are absorbed in the crystals.

To further examine the structure of the coumarin treated sample, the crystals were pressed gently onto the slide and examined by
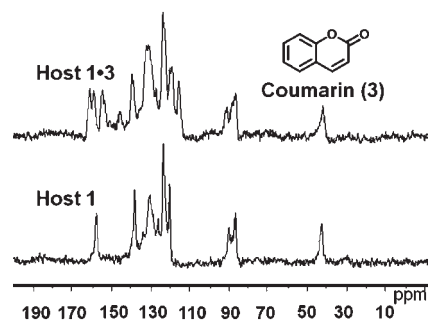
Figure 6. Solid-state cross polarized magic angle spinning ^{13}C {^{1}H} CP-MAS (125.79 MHz) NMR spectra for host **1** (bottom) and host **1·3** complex (top). Both spectra were acquired using a double resonant Doty Scientific XC 4 mm magic angle spinning (MAS) probe with TPPM modulated dipolar decoupling with a 61 kHz field strength.

Figure 7. (a) Solid-state UV−visibile absorption spectra of host **1**, host **1·coumarin**, and coumarin. (b) Comparison of the solid-state fluorescence spectra of host **1** (λ_{exc} =358 nm), **3** (λ_{exc} =351 nm), host **1·3** complex (λ_{exc} =347 nm).

PXRD (Figure 5b, ii). The host **1·3** displays a distinct PXRD pattern from host **1** (Figure 5b, i) and shows sharp and intense peaks consistent with a well ordered crystalline structure. Comparison of the PXRD patterns of the free host and the host **1·3** complex indicates that, in presence of the guest, there are changes in the long-range order of the host, but the complex remains highly crystalline.

We turned to solid-state NMR to compare the host and its coumarin complex. Solid-state cross polarized magic angle spinning ^{13}C {^{1}H} CP-MAS (125.79 MHz) NMR spectra were taken on the host before soaking and on the coumarin-treated host **1** (Figure 6). The treated host shows new peaks in the carbonyl (δ = 159.9, 153.5 ppm) and in the aromatic region that are consistent with coumarin, further supporting the hypothesis that coumarin was absorbed by the host. In addition, the cross-polarization build-up behavior of the coumarin is very similar to that of the resonances of the tube. This suggests that the mobility of the coumarin guest is similar to the columnar framework. These solid-state NMR and PXRD studies indicate that **3** is incorporated in the crystal lattice of host **1**.

We further examined the host **1·3** complex by optical methods. The host is only soluble in DMSO, an aggressive solvent that precludes complex formation. UV−visible absorption studies of a 1:1 mixture of host **1/3** in solution (2.5×10^{-5} M in DMSO) show only the expected bands for host **1** (λ_{max} = 286 and 305 nm) and coumarin **3** (λ_{max} = 276 and 321 nm) and no extra bands are apparent (see Figure S14 Supporting Information). UV−visible absorption studies of host **1**, **3**, and the host **1·3** complex were also examined in the solid-state using a Perkin-Elmer Lambda 35 UV/Visible scanning spectrophotometer equipped with an integrating sphere. Figure 7a shows that the host and the guest absorb in a similar range and have absorption maxima around 350 nm. The solid host−guest complex is a simple compilation of the two UV−visible absorbance spectra and no new bands are apparent.

We used fluorescence spectroscopy to further probe the interaction between the host and the guest. In solution, host **1** (2.5×10^{-6} M in DMSO) excited at λ_{exc} = 292 nm displays a broad fluorescence band with a maxima at 348 nm. Coumarin **3** does not fluoresce in DMSO solution and no changes are observed in the emission spectra of the host in the 1:1 mixture of host **1/3** in DMSO (Figure S25, Supporting Information). Excitation and emission spectra of ground solid samples of host **1**, **3**, and host **1·3** were recorded at room temperature using a Perkin-Elmer LS 55 Fluorescence Spectrometer. In each case, the excitation maximum
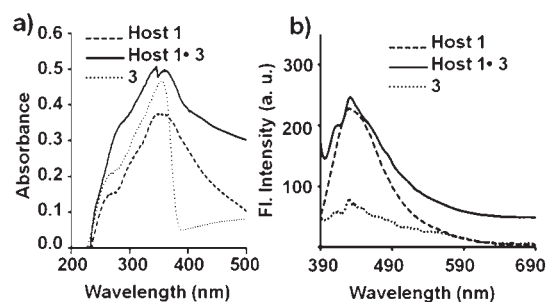
wavelength was used to generate the emission spectrum. Host **1**, **3**, and host **1·3** were excited at 358, 351, and 347 nm, respectively (Figure 7b). The solid-state fluorescence spectra of the host **1·3** complex (λ_{exc} = 347 nm) shows the expected bands at 408 nm (**3**) and 426 nm (host **1**), which suggest that coumarin has been indeed loaded within the host; however, once again, no new bands were observed.

We established that the host **1** crystals absorbed coumarin from solution to give a highly ordered solid complex (host **1·3**). Unfortunately, it is currently difficult to predict the molecular structure of the complex from the PXRD pattern. To gain further insight into the structure of the inclusion complex, we turned to molecular modeling using Spartan.[20] Molecular modeling studies allow us to probe the structure of the host **1·3** inclusion complex to examine the fit of coumarin inside the channel of **1** and to assess if host−guest interactions limit the number of accessible orientations a guest can sample inside the columnar structure. Specifically, we were interested in identifying any (1) interactions between the guests and the host framework and (2) interactions between neighboring coumarin molecules. We generated the host structure in Spartan using the atomic coordinates from the single crystal structure of host **1·nitrobenzene** and deleting coordinates of the nitrobenzene guests. The columnar framework was limited to four macrocycles, due to the increased size of this macrocycle as compared with our previous systems.[9b] The tetrameric host model was 'frozen' so that no movement was allowed in the column framework. A coumarin guest was added and allowed to move to energy minima in the static framework. Guests were added sequentially and minimized until no additional guest molecules could be accommodated. The host/guest ratio predicted by modeling studies was 1:1, which was slightly lower than the experimentally observed ratio. This might be due to edge effects given the small length of our model assembly as well as the fact that we are considering only an isolated column when in reality these are arrays of columns. In general, such calculations can suffer from such edge effect due to the small size of the modeled structure.[21]

Monte Carlo searching of the conformer distributions at ground state with Molecular Mechanics (MMFF) was performed to investigate the low energy conformers of the host **1·coumarin** complex. The Monte Carlo minimization program used a simulated annealing method to generate conformers of the host **1·3** inclusion complex.[22] We produced 450 conformers during the calculation, and the stabilization energy of the four lowest energy conformers fell within 0.5 kcal/mol. Each of these lowest energy structures showed the coumarin molecules organized
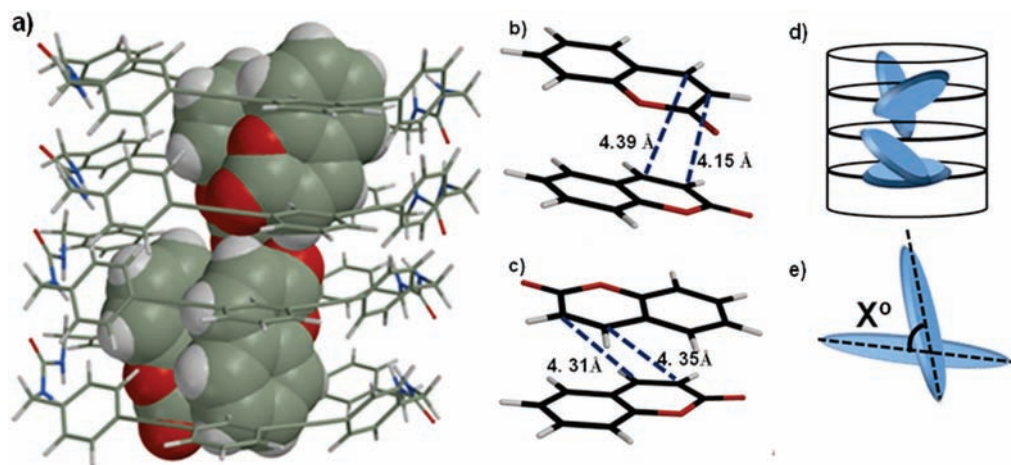
Figure 8. Models of the host **1·3** complex were constructed using Spartan. (a) Monte Carlo searching of the conformer distributions at ground state with molecular mechanics (MMFF) using Spartan generated this lowest energy structure. Host **1** was rendered in wire structures and **3** in space filling view. (b) View of the upper pair of coumarin molecules from part a; (c) view of the lower pair of coumarin molecules from part a; (d) schematic presentation of host **1·3** complex. (e) X° represents angle between the carbonyl groups of two adjacent coumarin units within the host channel. The planes formed by the carbonyl groups of the adjacent coumarins were not always parallel. X° varied significantly from 21 to 48° suggesting there is significant freedom of movement for the included guests.

**Scheme 2. Photolysis of Coumarin Affords Four Possible Products**
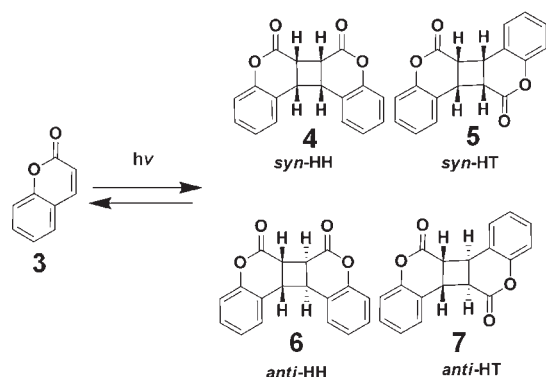
pairwise within the inclusion complex. The lowest energy conformer is shown in Figure 8a, which depicts the host framework in a wire view and guest molecules in a space filling view for clarity. It is notable that numerous edge to face aryl stacking interactions are predicted. These interactions hold the phenyl ring of **3** close to the phenyl rings in the wall of the host framework. These edge to face interactions range between 2.9 and 3.2 Å (from the center of the coumarin's benzene ring to the aryl hydrogen of the host framework). It is also notable that the packed coumarins interact not only with the column walls, but also with each other. Offset aryl stacking interactions stabilize the individual pairs of coumarins with the center-to-center distance between coumarin aryl rings ranging from 3.2 to 3.3 Å, typical distances for such stacking interactions.[23] Minimizations using different starting host—guest complex structures produced very similar sets of inclusion complex structures. Thus, our hypothesis is that coumarin can move within the host columns and that it is able to access a variety of geometries.

The photoreactions of coumarin are well-studied in both solution[24] and in the solid state, and are thought to require precise orientation and separation of the two reacting alkenes

between 3.6 and 4.2 Å.[25] Theoretically, UV-irradiation of coumarin may afford four possible dimers (Scheme 2): *syn*-head—head (HH) **4**, *syn*-head—tail (HT) **5**, *anti*-HH **6**, and *anti*-HT **7** in both solution and in the solid state. Solvent has a significant impact on both the percent conversion and selectivity of this photodimerization. High selectivity for the *anti*-HH **6** (91%) was observed for the reaction in benzene, albeit with low conversion (9%).[26] This product was also favored in the presence of triplet photosensitizers.[27] In contrast, photodimerization in polar solvents such as 1,2-ethanediol afforded higher conversion (39%) but lower selectivity (**4/5/6** = 59:19:22).[33] Photoreactions in the solid-state, however, typically show both low selectivity and limited conversion (<5%) due to their reversibility.[28] This reversibility is not true for the thermal reaction. A nice example of the thermal dimerization of coumarin from Wen et al. in a crystalline inclusion complex gives high selectivity (>95%) for the anti HH **6** at 30% conversion.[29]

Confinement within a solid host may limit molecular motion and change the selectivity of the photoreaction.[28b] For example, Ramamurthy found that **4** is favored in D_2O solution at 90% selectivity using a Fujita Pd nanocage.[32] Therefore, we analyzed the orientation of the two reactive alkenes in each of the coumarin pairs in the five lowest energy structures. The lowest energy conformer (Figure 8a) shows two pairs of coumarins (top and bottom) each held together by offset aryl stacking interaction. In the top pair, the reactive alkenes (Figure 8b) are oriented close together (average distance = 4.27 Å) but not exactly parallel to each other. Their carbonyl groups are in the same side, which would give rise to the *syn*-HH **4** photodimer after UV irradiation. The orientation of two coumarin molecules with respect to each other differs significantly in the bottom pair (Figure 8c). They are also held together by offset aryl stacking interactions; however, their carbonyl groups are located on opposite sides with the reactive alkenes relatively close in space (average distance = 4.33 Å). Thus, we would predict this orientation to form the *anti*-HT product **7**. The four lowest energy conformers of the host **1·3** complex are very close energetically, within 0.5 kcal/mol. All 10 coumarin pairs are organized by offset aryl stacking interactions and position their

Table 1. Comparison of Solid-State Photodimerization of Coumarin in the Presence or Absence of Host 1[a]

Entry	Host	Condition State/Atmosphere	Time (hour)	4:5:6:7	% Conv.
1	—	Solid / air	12	30:20:30:10	1-2
2	—	Solid / air	24	30:20:30:10	1-2
3	—	Solid / air	96	30:20:30:10	4-5
4	Host 1	Solid / air	12	<1:0:97:<1	8
5	Host 1	Solid / air	24	<1:0:97:<1	9
6	Host 1	Solid / air	96	<1:0:98:<1	18
7	Host 1	Solid/ N_2	12	<1:0:98:<1	11
8	Host 1	Solid/ N_2	24	<1:0:98:<1	16
9	Host 1	Solid/ N_2	96	<1:0:98:<1	37
10	Host 1	Solid/ Ar	12	<1:0:97:<1	19
11	Host 1	Solid/ Ar	24	<1:0:97:<1	26
12	Host 1	Solid/ Ar	96	<1:0:97:<1	55
13[b]	Pd cage	Soln / H_2O	10	>90:-:-:-	8
14[c]	—	Soln / HO~~OH	1	59:19:22:-	39
15[d]	—	Soln / ⬡	0.25	2:2:91:-	9

[a] Photodimerization in liquid media or in other hosts are shown in entries 13—15 for comparison. [b] In Pd-nanocage host, coumarin guest molecule was introduced from a solution of host and guest.[32] [c] In solution at a [3] = 0.5 mol/dm³.[26] [d] In solution [3] = 0.2 mol/dm³.[3,24,26]

reacting alkenes from 3.89 to 4.39 Å apart, favorable distances for the [2 + 2] reaction; however, the planes formed by the carbonyl groups of the adjacent coumarins were not always parallel, the favored alignment for reaction. However, the Ramamurthy group observed that photodimerization of coumarin is possible through [2 + 2] cycloaddition reaction in solid-state even when the two double bonds are not in parallel orientation.[30] A schematic presentation of coumarin pairs predicted by our models in the host 1·3 complex is shown in Figure 8d. If we define an angle (X°) between the planes of the included coumarins, we find this angle varies significantly from 21 to 48° (Figure 8e). Theoretically, the pairs could access three different photodimers (syn-HH 4, anti-HH 6, and anti-HT 7). Overall, the molecular modeling analysis suggested that pairs of 3 would be packed close enough to undergo [2 + 2] photodimerization reactions; however, their exact orientation might not be controlled enough to give high selectivity.

Given these predictions, we set out to test if coumarin in the complex would react under UV-irradiation with particular emphasis on the reaction conversion and on its selectivity. The host 1·3 complex (30 mg) in Norell S-5-500-7 NMR tubes with 100% transmittance up to 400 nm was irradiated at room temperature in air using a Hanovia 450 W medium pressure mercury arc lamp cooled in a quartz immersion well that allows broad spectrum UV transmittance (200—400 nm). Samples (5 mg) were removed after 12, 24, and 96 h for analysis. The photoproducts were separated from the host by extraction with $CDCl_3$ and analyzed by ^{1}H NMR spectroscopy. The conversion was estimated by comparison of the starting material (at 6.42 ppm) to the cyclobutyl CH's (δ 3.5—4.4 ppm). For the 12 h sample, we observe only one photodimer, which is the anti-HH 6 in 8% conversion with 97% selectivity (Table 1, entry 4). The exclusive production of anti-HH photodimer in the solid state was both unexpected and unprecedented. In general, the solid-state photoirradiation of solid coumarin provides dimers with no selectivity (Table 1, entries 1—3) and low conversion (<5%), a fact that is usually attributed to the reversibility of this reaction under

continued irradiation.[25] Direct dissolution of the samples in DMSO-d_6 gave similar results, indicating that the products were efficiently removed from the crystals by washing. Longer reaction times did not change the selectivity of the product but increased the conversion. Photoirradiation for 24 and 96 h afforded the same photodimer 6 with 97—98% selectivity in 9% and 18% conversion, respectively. This selective solid-state dimerization of coumarin was quite surprising and led us to further probe if this molecular cage might be facilitating dimer formation, slowing the reverse reaction of the dimer back to coumarin or alternatively displaying a thermodynamic preference for the bound product 6.

The atmosphere is known to affect the conversion of coumarin to its photodimers. Oxygen can quench the excited state of coumarin and limit conversion.[31] Our gas absorption data demonstrated that the host channels were accessible to CO_2 (g), while molecular modeling studies suggested that the channels should be large enough to accommodate a number of different gases including O_2 (g), N_2 (g), or Ar (g). To test whether coumarin was accessible to the atmosphere in the solid complex, we investigated the reaction under inert atmospheres (N_2 (g) and Ar (g)). Surprisingly, reaction under a N_2 (g) atmosphere gave similarly high selectivity (98% of 6) with slightly higher conversion at 12 h (Table 1, entry 7). Longer irradiation times of 24 and 96 h afford increased conversion (16% and 37%) with 97—98% selectivity for photodimer 6. The conversion could be further enhanced under Ar (g) to yield 55% conversion at 96 h (Table 1, entries 10—12) with no decrease in selectivity (97%). The observed increase in conversion under inert gases suggests that the coumarin absorbed in the solid complex is still accessible to quenching by oxygen in the air atmosphere. The 55% conversion limit may be due to lack of uniform irradiation of the crystals or inefficient light penetration. We are currently investigating methods for grinding the host—guest complex and irradiating the powder or alternatively, irradiating a suspension of the powder in a deoxygenated solvent.

We observed unexpected and unusually high conversion and selectivity for the anti-HH photodimer 6 in the solid state. This anti-HH photodimer is observed in solution via the triplet excited state in presence of photosensitizer like benzophenone. This leads us to the question of whether our host is acting as a triplet photosensitizer in the solid state or if this product is a result of confinement effects. Absorption and emission spectra of the solid host 1·3 complex do not support triplet sensitization; however, it is unfortunately very difficult in the solid-state to probe if the fluorescence lifetimes are altered by the host—guest complexation. To address this issue, we turned to an experimental approach with the assumption that if the host were able to act as a photosensitizer this effect should also be observed in solution. Coumarin (25 mM) was UV-irradiated in the presence and absence of host 1 (1.5 equiv) in d_6-DMSO, where host 1 is soluble as well as in d_6-benzene, where host 1 is insoluble. The coumarin (25 mM in benzene) was similarly UV-irradiated in the presence and absence of the more soluble host 2 (Scheme 1), which contains protected ureas. Host 2 is soluble in benzene, which is generally a better solvent for this reaction. As additional controls, coumarin was photoirradiated under the same condition in the presence and absence of benzophenone, a known triplet sensitizer. No conversion of coumarin was observed in either solvent in the presence of either host 1 or its soluble analogue 2, while benzophenone facilitates the conversion of coumarin 17% (after 12 h) to the anti-HH photodimer, similar to

prior reports.[33] In addition, neither host **1** or **2** facilitates the photoisomerization of *trans-β*-methyl styrene (Supporting Information), a reaction known to require a low energy triplet sensitizer.[34] These experiments along with the solid-state emission spectra suggest that the production of the *anti*-HH photodimer is not due to triplet sensitization by a single host molecule and may be due to encapsulation within the larger assembly.

In summary, we report the synthesis and self-assembly of a macrocyclic bis-urea that contains a much larger phenylethynylene spacer unit. Despite its increased size, this bis-urea macrocycle still assembles in high fidelity to give columnar structures that pack into porous crystalline materials. The porosity of these new materials was demonstrated by gas adsorption studies and by the absorption of coumarin guests from solution. Modeling studies including Monte Carlo searching of the conformer distributions at ground state with molecular mechanics (MMFF) using Spartan did not afford good predictions about the selectivity of the subsequent photoreaction; however, they did suggest that the coumarin binds in pairs through advantageous aryl stacking interactions with the interior of the columns and that the pairs of coumarins have room to move within the channel. We demonstrated the utility of this new porous framework as a confined environment for reactions with the solid-state photodimerization of coumarin within the solid host−guest complex. UV-irradiation of host **1**·coumarin afforded the *anti*-HH coumarin photodimer with unusually high selectivity. Longer UV-irradiation times resulted in higher conversion, in contrast to what is typically observed in solid-state photoreaction of coumarin, which gives limited conversion due to the photoreversion of the photodimer to coumarin. We are currently exploring the uptake and subsequent photoreaction of larger coumarin and stilbene derivatives that may be better matched to the size and shape of the channel. We are also investigating the crystallization of host **1** in the presence of coumarin to see if we can grow crystalline inclusion complexes suitable for X-ray crystallography. Such structural characterization will help to evaluate the accuracy of our molecular models. X-ray analysis of such inclusion crystals after intervals of UV-irradiation might reveal the course of events between light absorption and guest reaction and help to determine the origin of the observed selectivity.

■ ASSOCIATED CONTENT

⑤ Supporting Information. Synthesis and characterization of host **1** and its inclusion complexes; photochemical reaction of coumarin in the presence and absence of host **1**, and X-ray crystallographic files in CIF format for **1**. This material is available free of charge via the Internet at http://pubs.acs.org.

■ AUTHOR INFORMATION

Corresponding Author
shimizul@chem.sc.edu

■ ACKNOWLEDGMENT

■ REFERENCES

(1) (a) Vriezema, D. M.; Aragones, M. C.; Elemans, J. A. A. W.; Cornelissen, J. J. L. M.; Rowan, A. E.; Nolte, R. J. M. *Chem. Rev.* **2005**, *105*, 1445–1489. (b) Koblenz, T. S.; Wassenaar, J.; Reek, J. N. H. *Chem. Soc. Rev.* **2008**, *37*, 247–262.

(2) (a) Tung, C. H.; Wu, L. Z.; Zhang, L. P.; Chen, B. *Acc. Chem. Res.* **2003**, *36*, 39–47. (b) Yang, Q.; Han, D.; Yang, H.; Li, C. *Chem.—Asian J.* **2008**, *3*, 1214–1229.

(3) (a) Fukuda, T.; Yamauchi, S.; Honda, Z. *Opt. Mater.* **2009**, *32*, 207–211. (b) Crescimbeni, M. C.; Nolan, V.; Clop, P. D.; Marin, G. N.; Perillo, M. A. *Colloids Surf., A* **2010**, *76*, 387–396. (c) Kin, E.; Fukuda, T.; Yamauchi, S.; Honda, Z.; Ohara, H.; Yokoo, T.; Kijima, N.; Kamata, N. *J. Alloys Compd.* **2009**, *480*, 908–911. (d) Gill, I.; Ballesteros, A. *J. Am. Chem. Soc.* **1998**, *120*, 8587–8598.

(4) (a) Murase, F.; Horiuchi, S.; Fujita, M. *J. Am. Chem. Soc.* **2010**, *132*, 2866–2867. (b) Yoshizawa, M.; Klosterman, J. K.; Fujita, M. *Angew. Chem., Int. Ed.* **2009**, *48*, 3418–3438. (c) Iwasawa, T.; Hooley, R. J.; Rebek, J., Jr. *Science* **2007**, *317*, 493–496. (d) Ziegler, M.; Brumaghim, J. L.; Raymond, K. N. *Angew. Chem., Int. Ed.* **2000**, *39*, 4119–4121. (e) Iwasawa, T.; Mann, E.; Rebek, J. *J. Am. Chem. Soc.* **2006**, *128*, 9308–9309. (f) Fiedler, D.; Bergman, R. G.; Raymond, K. N. *Angew. Chem., Int. Ed.* **2004**, *43*, 6748–6751. (g) Yoshizawa, M.; Kusukawa, T.; Fujita, M.; Yamaguchi, K. *J. Am. Chem. Soc.* **2000**, *129*, 6311–6312. (h) Chen, J.; Rebek, J., Jr. *Org. Lett.* **2002**, *4*, 327–329. (i) Mal, P.; Breiner, B.; Rissanen, K.; Nitschke, J. R. *Science* **2009**, *324*, 1697–1699. (j) Butterfield, S. M.; Rebek, J., Jr. *Chem. Commun.* **2007**, 1605–1607. (k) Sato, S.; Iida, J.; Suzuki, K.; Kawano, M.; Ozeki, T.; Fujita, M. *Science* **2006**, *313*, 1273–1275. (l) Cram, D. J.; Tanner, M. E.; Thomas, R. *Angew. Chem., Int. Ed. Engl.* **1991**, *30*, 1024–1027. (m) Yoshizawa, M.; Fujita, M. *Pure Appl. Chem.* **2005**, *77*, 1107–1112.

(5) (a) Lakshminarasimhan, P.; Thomas, K. J.; Brancaleon, L.; Wood, P. D.; Johnston, L. J.; Ramamurthy, V. *J. Phys. Chem. B* **1999**, *103*, 9247–9254. (b) Jayathirtha, R. V.; Prevost, N.; Ramamurthy, V.; Kojima, M.; Johnston, L. J. *Chem. Commun.* **1997**, *22*, 2209–2210.

(6) (a) Yoshizawa, M.; Tamura, M.; Fujita, M. *J. Am. Chem. Soc.* **2004**, *126*, 6846–6847. (b) Pluth, M. D.; Bergman, R. G.; Raymond, K. N. *Science* **2007**, *316*, 85–87. (c) Sato, S.; Iida, J.; Suzuki, K.; Ozeki, T.; Fujita, M. *Science* **2007**, *313*, 1273–1276. (d) Murase, T.; Sato, S.; Fujita, M. *Angew. Chem., Int. Ed.* **2007**, *46*, 1083–1085. (e) Kawano, M.; Kobayashi, Y.; Ozeki, T.; Fujita, M. *J. Am. Chem. Soc.* **2006**, *128*, 6558–6559. (f) Dong, V. M.; Fiedler, D.; Carl, B.; Bergman, R. G.; Raymond, K. N. *J. Am. Chem. Soc.* **2006**, *128*, 14464–14465. (g) Rebek, J., Jr.; Ajami, D. *Proc. Natl. Acad. Sci. U.S.A.* **2007**, *104*, 16000–16003. (h) Pluth, M. D.; Bergman, R. G.; Raymond, K. N. *Science* **2007**, *316*, 85–88. (i) Pluth, M. D.; Fiedler, D.; Mugridge, J. S.; Bergman, R. G.; Raymond, K. N. *Proc. Natl. Acad. Sci. U.S.A.* **2009**, *26*, 10438–10443. (j) Balomenou, I.; Pistolis, G. *J. Phys. Chem. B* **2010**, *114* (2), 780–785. (k) Yoshizawa, M.; Kusukawa, T.; Fujita, M.; Yamaguchi, K. *J. Am. Chem. Soc.* **2000**, *122*, 6311–6312.

(7) (a) Chretien, M. N. *Pure Appl. Chem.* **2007**, *79*, 1–20. (b) Hashimoto, S. *J. Photochem. Photobiol., C* **2003**, *4*, 19–49. (b) Garcia, H.; Roth, H. D. *Chem. Rev.* **2002**, *102*, 3947–4007. (c) Yoon, K. B. *Chem. Rev.* **1993**, *93*, 321–339.

(8) Shimizu, L. S.; Smith, M. D.; Hughes, A. D.; Shimizu, K. D. *Chem. Commun.* **2001**, 1592–1593.

(9) (a) Yang, J.; Dewal, M. B.; Shimizu, L. S. *J. Am. Chem. Soc.* **2006**, *128*, 8122–8123. (b) Yang, J.; Dewal, M. B.; Profeta, S.; Smith, M. D.; Li, Y.; Shimizu, L. S. *J. Am. Chem. Soc.* **2008**, *130*, 612–621. (c) Dewal, M. B.; Xu, Y.; Yang, J.; Mohammed, F.; Smith, M. D.; Shimizu, L. S. *Chem. Commun.* **2008**, 3909–3911.

(10) (a) Feng, X.; Liu, L.; Wang, S.; Zhu, D. *Chem. Soc. Rev.* **2010**, *39*, 241102419. (b) Dore, K.; Leclerc, M.; Boudreau, D. *J. Fluoresc.* **2006**, *16*, 259–265.

(11) (a) Thomas, S. W.; Joly, G. D.; Swager, T. M. *Chem. Rev.* **2007**, *107*, 1339–1386. (b) Pecher, J.; Mecking, S. *Chem. Rev.* **2010**,

110, 6260–6279. (c) McQuade, D. T.; Pullen, A. E.; Swager, T. M. *Chem. Rev.* **2000**, *100*, 2537–2574.

(12) (a) Mangel, T.; Eberhardt, A.; Scherf, U.; Bunz, U. H. F.; Mullen, K. *Macromol. Rapid Commun.* **1995**, *16*, 571–580. (b) Nelson, J. C.; Saven, J. G.; Moore, J. S.; Wolynes, P. G. *Science* **1997**, *277*, 1793–1796. (c) Brunsveld, L.; Meijer, E. W.; Prince, R. B.; Moore, J. S. *J. Am. Chem. Soc.* **2001**, *123*, 7978–7984.

(13) (a) Zhao, D.; Moore, J. S. *Chem. Commun.* **2003**, 807–818. (b) Zhu, A.; Bharathi, P.; Drickamer, H. G.; Moore, J. S. *J. Polym. Sci., Part A: Polym. Chem.* **2001**, *39*, 2859–2865. (c) Zhu, A.; Bharathi, P.; White, J. O.; Drickamer, H. G.; Moore, J. S. *Macromolecules* **2001**, *34*, 4606–4609. (d) Swallen, S. F.; Kopelman, R.; Moore, J. S.; Devadoss, C. *J. Mol. Struct.* **1999**, *485*, 585–597. (e) Buchko, C. J.; Wilson, P. M.; Xu, Z.; Zhang, J.; Moore, J. S.; Martin, D. C. *Polymer* **1995**, *36*, 1817–1825.

(14) (a) Hoger, S.; Morrison, D. L.; Enkelmann, V. *J. Am. Chem. Soc.* **2002**, *124*, 6734–6736. (b) Hoeger, S. *J. Polym. Sci., Part A: Polym. Chem.* **1999**, *37*, 2685–2698.

(15) (a) Luo, J.; Yan, Q.; Zhou, Y.; Li, T.; Zhu, N.; Bai, C.; Cao, Y.; Wang, J.; Pei, J.; Zhao, D. *Chem. Commun.* **2010**, *46*, 5725–5727. (b) Yamaguchi, Y.; Yoshida, Z. *Chem.—Eur. J.* **2003**, *9*, 5430–5440. (c) Grave, C.; Schluter, A. D. *Eur. J. Org. Chem.* **2002**, 3075–3098.

(16) Zang, L.; Che, Y. K.; Moore, J. S. *Acc. Chem. Res.* **2008**, *41*, 1596–1608.

(17) Laugier, J.; Bochu, B. POUDRIX, a suite of programs for the interpretation of X-ray experiments, ENSP/LMGP, BP 46, 38042 Sain Martin d'Hères, France, 2000, http://www.inpg.fr/LMPG and http://www.ccp14.ac.uk/tutorial/lmgp/poudrix.htm.

(18) (a) Barton, T. J.; Bull, L. M.; Klemperer, W. G.; Loy, D. A.; McEnaney, B.; Misono, M.; Monson, P. A.; Pez, G.; Schere, G. W.; Varuli, J. C.; Yaghi, O. M. *Chem. Mater.* **1999**, *11*, 2633–2656. (b) Groen, J. C.; Peffer, L.; Perez-Ramirez, J. A. *Microporous Mesoporous Mater.* **2003**, *60*, 1–17.

(19) Wang, R.; Bardelang, D.; Waite, M.; Udachin, K. A.; Leek, D. M; Yu, K.; Ratcliffe, C. I.; Ripmeester, J. A. *Org. Biomol. Chem.* **2009**, *7*, 2435–2439.

(20) *Spartan 04 for Macintosh*, V. 1.1.1.;Wavefunction, Inc.: Irvine, CA, 2007.

(21) Sieval, B. A.; Hout, B. V. D.; Zulihof, H.; Sudholter, E. J. R. *Langmuir* **2001**, *17*, 2172–2181.

(22) (a) Kzos, J. S.; Sommer, J. U. *Macromolecules* **2009**, *42*, 4878–4886. (b) Meirovitch, H.; Vasquez, M. *J. Mol. Struct.* **1997**, *398—399*, 517–522.

(23) (a) Meyer, E. A.; Castellano, R. K.; Diederich, F. *Angew. Chem., Int. Ed.* **2003**, *42*, 1210–1250. (b) Coates, G. W.; Dunn, A. R.; Henling, L. M.; Dougherty, D. A.; Grubbs, R. A. *Angew. Chem., Int. Ed. Engl.* **1997**, *36*, 248–251.

(24) (a) Krauch, H.; Farid, S.; Schenck, G. O. *Chem. Ber.* **1966**, *99*, 625–631. (b) Hoffman, R.; Wells, P.; Morrison, H. *J. Am. Chem. Soc.* **1971**, *36*, 102–107.

(25) (a) Vishnumurthy, K.; Guru Row, T. N.; Venkatesan, K. *J. Chem. Soc., Perkin Trans. 2* **1997**, 615–619. (b) Vishnumurthy, K.; Guru Row, T. N.; Venkatesan, K. *J. Chem. Soc., Perkin Trans. 2* **1996**, 1475–1478. (c) Craig, D. P.; Mallet, C. P. *Chem. Phys.* **1982**, *65*, 129–142. (d) Craig, D. P.; Lindsay, R. N.; Mallet, C. P. *Chem. Phys.* **1984**, *89*, 187–197. (e) Bhadbhade, M. M.; Murthy, G. S.; Venkatesan, K.; Ramamurthy, V. *Chem. Phys. Lett.* **1984**, *109*, 259–263. (f) Gnanaguru, K.; Murthy, G. S.; Venkatesan, K.; Ramamurthy, V. *Chem. Phys. Lett.* **1984**, *109*, 255–258.

(26) Yu, X.; Scheller, D.; Rademacher, O.; Wolff, T. *J. Org. Chem.* **2003**, *68*, 7386–7399.

(27) Morrison, H.; Curtis, H.; McDowell, T. *J. Am. Chem. Soc.* **1966**, *88*, 5415–5419.

(28) (a) Gnanaguru, K.; Ramasubbu, N.; Venkatesan, K.; Ramamurthy, V. *J. Org. Chem.* **1985**, *50*, 2337–2346. (b) Tanaka, K.; Toda, F. *Chem. Rev.* **2000**, *100*, 1025–1074. (c) Barooah, N.; Pemberton, B. C.; Sivaguru, J. *Org. Lett.* **2008**, *10*, 3339–3342.

(29) Wen, Y.; Song, Y.; Zhao, D.; Ding, K.; Bian, J.; Zhang, X.; Wang, J.; Liu, Y.; Jiang, L.; Zhu, D. *Chem. Commun.* **2005**, 2732–2734.

(30) (a) Murthy, G. S.; Arjunan, P.; Venkatesan, K.; Ramamurthy, V. *Tetrahedron* **1987**, *43*, 1225–40. (b) Bhadbhade, M. M.; Murthy, G. S.; Venkatesan, K.; Ramamurthy, V. *Chem. Phys. Lett.* **1984**, *109*, 259–263.

(31) (a) Pemberton, B. C.; Barooah, N.; Srivatsava, D. K.; Sivaguru, J. *Chem. Commun* **2010**, *46*, 225–227.(b) Turro, N. J. . In *Modern Molecular Photochemistry*; University Science Books: Sausalito, CA, 1991; pp 462—464. (c) Lewis, F. D.; Barancyk, S. V. *J. Am. Chem. Soc.* **1989**, *111*, 8653–8661. (d) Lewis, F. D.; Howard, D. K.; Oxman, J. D. *J. Am. Chem. Soc.* **1983**, *105*, 3344–3345. (e) Moorthy, J. N.; Venkatesan, K.; Weiss, R. G. *J. Org. Chem.* **1992**, *57*, 3292–3297. (f) Muthuramu, K.; Ramnath, N.; Ramamurthy, V *J. Org. Chem.* **1983**, *48*, 1872–1876. (h) Wolff, T.; Görner, H. *J. Photochem. Photobiol., A* **2010**, *209*, 219–223.

(32) Karthikeyan, S.; Ramamurthy, V. *J. Org. Chem.* **2006**, *71*, 6409–6413.

(33) Wolff, T.; Gorner, H. *Phys. Chem. Chem. Phys.* **2004**, *6*, 368–376 and references therein.

(34) (a) Arai, T.; Sakuragi, H.; Tokumaru, K. *Bull. Chem. Soc. Jpn.* **1982**, *55*, 2204. (b) Rockley, M. G.; Salisbury, K. *J. Chem. Soc. Perkin Trans. 2* **1973**, 1582.